Molecular Forces between Membranes Displaying Neutral Glycosphingolipids: Evidence for Carbohydrate Attraction†

Z. W. Yu, T. L. Calvert, and D. Leckband*

Department of Chemical Engineering, University of Illinois at Urbana−Champaign, 600 S. Mathews Ave., Urbana, Illinois 61801

Received April 30, 1997; Revised Manuscript Received November 17, 1997

ABSTRACT: The surface force apparatus was used to determine the fundamental forces governing the adhesion between mixed bilayer membranes comprising lactosyl ceramide (LacCer) and di-tridecanoyl-phosphatidyl choline. Forces between membranes were quantified as a function of the glycolipid surface densities, which ranged from 0 to 30 mol %. Control measurements of the forces between pure phosphatidylcholine membranes and mixed bilayers of lactosyl ceramide with phosphocholine showed that the steric thickness of the carbohydrate headgroups increased from 19 to 25 Å when the glycolipid density increased from 10 to 20 mol %. The layer compressibility also decreased with increasing carbohydrate coverage, but the corresponding adhesion between lactosyl ceramide-containing membranes increased with increasing amounts of glycosphingolipid in them. The nonspecific van der Waals forces accounted for the attraction measured in the control experiments and that between identical 10 mol % LacCer bilayers. However, the increase in the adhesion with increasing glycolipid density was 2−4 times greater than predicted by Lifschitz theory. Additionally, the forces measured during separation of membranes containing 20 and 30 mol % glycosphingolipid indicated that the headgroups bind and rearrange during bilayer detachment. The interactions between the carbohydrates are weak and apparently dynamic, and they generate an additional density-dependent intermembrane attraction that is on the order of the van der Waals force.

The biological function of glycosphingolipids (GSLs)[1] on cell membranes has been of interest for many years (*1*−*3*). Significant changes in both the densities and identities of GSLs on cell surfaces are associated with various disease states, with cellular differentiation, development, and with oncogenesis. Such correlations suggest that glycolipids likely play key roles in cell recognition and adhesion. Consistent with this notion, GSLs have been known to block intercellular recognition during morphogenesis and histogenesis (*1*).

In cell−cell adhesion studies, carbohydrate-mediated attachment is typically assumed to involve interactions between definite carbohydrate structures and cognate receptor proteins such as lectins (*3*). Interactions between L-selectin and oligosaccharides, for example, support lymphocyte homing on the postcapillary endothelial cells. E-selectin similarly mediates carbohydrate-dependent myeloid cell adhesion to activated endothelium (*4*). Biophysical studies also demonstrated that differences in the selectin-carbohydrate bond strengths control leukocyte rolling and arrest during inflammation (*5*). Interactions between various proteins and cell surface carbohydrates are common mechanisms of cell signaling and adhesion. In one of the more frequently cited cellular recognition processes, the sperm-egg interaction, carbohydrates are believed to play a fundamental role as mediators (*6*).

In addition to lectin-mediated cell adhesion, interactions between carbohydrates themselves have been implicated in cellular attachment. The pioneering work by Hakomori and co-workers suggests that binding between specific GSL moieties on cell surfaces indeed plays an important role in the initial adhesion events (*7*, *8*). They proposed that the fairly uniform distribution of glycosphingolipids over cell surfaces may mediate weak, early adhesive contacts, prior to the recruitment of stronger-binding protein receptors into the contact region (*1*, *8*). Correlations of cell attachment strengths with the expression levels of various GSLs provide strong evidence that both homotypic and heterotypic glycolipid interactions promote cell adhesion. For example, the mouse B16 melanoma cell line, a high expressor of the monoganglioside GM_3, binds specifically to mouse lymphoma L5178 AA12 cells, which express high levels of gangliotriaosylceramide (Gg_3). The strong adhesion of the two cell types can be inhibited by monoclonal antibodies against either of the latter gangliosides (*8*, *9*). The heterotypic interaction between these negatively charged species is also calcium dependent. By contrast, homotypic, specific binding between multivalent sialyl $Lewis^x$, was also reported (*7*).

More recently, lateral interactions between GSLs within the cell membrane were implicated in the formation of caveolae and membrane microdomains or rafts composed

† This work was supported by the National Institutes of Health (GM51338) and by a CAREER award from the National Science Foundation (BES 9503045).

* To whom correspondence should be addressed.

[1] Abbreviations: SFA, surface force apparatus; LacCer, lactosyl ceramide (Galβ1−4Glcβ1−1Cer); GSL, glycosphingolipid; DTPC, 1, 2-di-tridecanoylphosphatidylcholine; DMPC, 1, 2-di-myristoylphosphatidylcholine; DPPE, 1, 2-dipalmitoylphosphatidylethanolamine.

S0006-2960(97)01010-6 CCC: $15.00
Published on Web 01/22/1998

of GSLs and GPI-anchored proteins (*10*). The glycosphingolipids can associate into patches when mixed with other lipids (*11*). These aggregate structures are hypothesized to play important roles in protein processing, localization, and transmembrane signaling (*10*, *12*−*14*). Furthermore, the localization of glycosylphosphatidyl inositol (GPI)-linked proteins in these GSL-rich rafts (*10*, *15*) may be associated with the preferential glycosphingolipid enrichment of the apical surface of kidney cells (*16*). The aggregates were identified by detergent extraction (*10*) and indirectly by single-particle tracking on cell membranes (*17*). Studies by Schroeder et al. (*18*) suggest that interactions between the acyl chains may stabilize these aggregates against detergent. However, the self-assembly of amphiphilic aggregates typically involves interactions between both the headgroups and tails (*19*). Still in question, therefore, is the nature of the interactions between the headgroups. A recent investigation of the isotherms of pure glycolipid monolayers at the air−water interface provided the first demonstration of lateral attractive interactions between glycosphingolipids, on the basis of the negative mixing enthalpy of the GSLs in phosphatidylcholine matrixes (*20*).

Attractive interactions between the carbohydrate headgroups have, however, not been measured directly. Additionally, the forces that mediate intermembrane adhesion and lipid clustering are likely to be linked to both the GSL surface concentration and to the carbohydrate structures. These are intriguing issues, but there is still little physical evidence for the existence of attractive forces between glycolipids on interacting cell membranes or between those contained in such aggregates.

To elucidate the molecular interactions that may mediate these events, both the surface force apparatus and osmotic stress techniques were used to quantify directly the ranges and magnitudes of the molecular forces between glycolipid-phospholipid mixtures (*21*−*26*). The latter investigations, however, focused primarily on interactions between negatively charged GSLs in the absence of calcium. Forces between bilayers of GM_1 or of G_{T1b} mixed with phosphatidylcholines were repulsive, due to the strong electrostatic double-layer force and shorter-range steric repulsion between the charged surfaces. Interestingly, Luckham et al. (*25*) reported an unusually large adhesion between the mixed phosphatidylcholine-glycosphingolipid membranes, which they attributed to attractive interactions between the carbohydrate and the choline headgroups. Similarly, the apparent Hamaker constants between phospholipid membranes containing neutral glycolipid were unexpectedly high (*26*). However, in none of these cases did the authors investigate the possibility of direct binding between the carbohydrate headgroups.

In this paper, we present direct surface force measurements of attractive interactions between uncharged lipid bilayers containing the neutral glycosphingolipid, lactosyl ceramide (LacCer, Figure 1). The latter GSL reportedly mediates cell adhesion via calcium-dependent, heterotypic binding to the sialylated glycolipid GM_3 (*1*). Moreover, due to the lack of charge, the origins of the attractive forces between glycosphingolipid-containing bilayers were more easily studied. To identify the origins of the measured intermembrane adhesion, we conducted force measurements between membranes containing 0, 10, 20, and 30 mol % LacCer. While the van der Waals force, as determined by Lifschitz theory, can account for the measured adhesion at low GSL coverage, the increase in adhesion with increasing LacCer density was too large to be attributed to the van der Waals force alone. Differences between the force profiles measured during the approach and separation of membranes containing high LacCer concentrations gave direct evidence for binding between the carbohydrate headgroups. These results suggest that the lactosyl headgroups enhance the intermembrane adhesion through the formation of attractive, presumably nonspecific interactions between the opposed carbohydrates. It follows that glycolipids do not present strictly repulsive cell membrane surface barriers, but can augment the intermembrane attraction. Such forces may also operate between adjacent carbohydrates within the same membrane and thus influence bilayer organization.

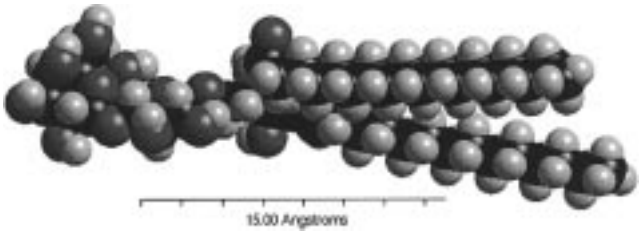

FIGURE 1: Space filling model of the stearoyl derivative of lactosyl ceramide.

MATERIALS AND METHODS

Chemicals. Lactosyl ceramide (Galβ1−4Glcβ1−1Cer; from bovine brain, stearoyl derivative, molecular weight 889) was purchased from Matreya, Inc. (Pleasant Gap, PA). 1,2-Dipalmytoylphosphatidylethanolamine (DPPE) and 1,2-ditridecanoylphosphatidylcholine (DTPC) was from Avanti (Alabaster, AL). The tri-ethylammonium salt of Texas Red DHPE was acquired from Molecular Probes, Inc. Sodium nitrate (analytical reagent) was from Mallinckrodt, Inc. (Kentucky).

Mixtures of the glycosphingolipid and phospholipid were prepared by mixing the appropriate quantities of the stock lipids in chloroform/methanol solutions. The stock lactosyl ceramide solutions and mixtures were never kept for more than 2 weeks. For these investigations, we used DTPC as the matrix lipid on account of its melting temperature (T_m = 14 °C) and the stability of DTPC monolayers at the air−water interface at 25 °C. The melting temperature ensured the fluidity of the DTPC lipids at the measurement temperature of 25 °C. By contrast, DLPC monolayers (T_m = −1 °C) were less stable due to the greater solubility of the latter lipid. Similarly, the melting temperature of DMPC (T_m = 23 °C) was too near the temperature of the measurements. As shown below, however, the properties of the DTPC monolayers were as expected for phosphatidyl cholines.

Differential Scanning Calorimetry. Calorimetry measurements were performed with a Perkin-Elmer DSC-7 calorimeter, operated at a scanning rate of 5 deg/min. Lipid mixtures of DTPC and LacCer that contained either 10 or 20 mol % LacCer were first dissolved in a mixed solvent of chloroform and methanol (2:1, vol/vol). Solvents were evaporated under nitrogen. After further removing trace solvents by storing the samples under vacuum overnight, the lipid mixtures were fully hydrated with either water purified with a MilliQ-UF

system (Millipore) or an aqueous salt solution containing 20 mM sodium nitrate. The lipid-to-solution ratio was about 1/6. We prepared lipid dispersions by cycling the lipids several times between −20 and 40 °C and dispersing the lipids by extensive vortexing between the thermal cycles.

Surface Force Apparatus (SFA) Measurements. With the surface force apparatus, one measures the molecular forces between materials supported on two macroscopic, perpendicular cylinders as a function of their separation distance (*27*). The intersurface separations are determined with a resolution of ±1 Å by optical interferometry (*28*). The force between the interacting materials is determined from the deflection of a sensitive spring, which supports one of the two cylindrical lenses supporting the samples. The force resolution is typically ±10 nN (*29*).

Force measurements were obtained with a Mark II surface force apparatus and with an SFA3 instrument (SurForce Corp., Santa Barbara, CA), both of which were interfaced with a Jarrell Ash monochromator and video recording system. Data were taken at 25 °C.

We prepared supported bilayer membranes by the Langmuir−Blodgett (LB) deposition of lipid monolayers from the water−vapor interface of a Langmuir trough (NIMA; Coventry, England) onto freshly cleaved mica supports, according to published procedures (*30*, *31*). The first layer consisted of a solid, crystalline monolayer of DPPE. The deposition was carried out at 35 mN/m and a mean molecular area of 43 Å^2/lipid. The second, outer LB-monolayer, the working monolayer, was a binary mixture of lactosyl ceramide and DTPC. The mixtures contained either 10, 20, or 30 mol % LacCer. The latter lipids were spread at the water−vapor interface and compressed to 35 mN/m, which corresponds to an average molecular area of 67 Å^2/lipid at 25 °C. The deposition onto DPPE was done at a constant pressure of 35 mN/m. The transfer ratio for both distal and proximal layers, that is, the ratio of the lipid area transferred to the surface area coated, exceeded 0.95 in all the experiments. The coated disks were then transferred under water to the chamber of the apparatus, and mounted. The chamber contained 20 mM $NaNO_3$ that was saturated with DTPC monomers.

Vesicle Adsorption Measurements. In these measurements, we determined qualitatively the impact of membrane-bound carbohydrate on the adsorption of multilamellar lipid vesicles, composed of LacCer and DTPC, onto supported planar bilayers of similar or identical composition. The supported planar bilayers were deposited on both sides of freshly cleaved 1 × 2 cm^2 mica sheets, exactly as described for the SFA samples. The outer layer of the supported bilayer contained 10 or 20 mol % LacCer in a DTPC matrix, and the lower layer was DPPE.

Fluorescently labeled, multilamellar vesicles consisted of either pure DTPC or of LacCer/DTPC mixtures, together with 3 mol % Texas Red dihexadecyl phosphatidylethanolamine (TR-DHPE, Molecular Probes). The lipid mixture was first dissolved in a mixture of chloroform/methanol (3/1, v/v). We evaporated the solvent by passing a stream of nitrogen over the lipid solution until a thin crust was left on the wall of the test tube. The addition of pure water hydrated the latter film, and vortexing for 1 min dispersed the vesicles. The resulting suspension was sonicated for about 1 h. An aliquot of the multilamellar vesicle suspension thus prepared was added immediately to the test tubes containing the supported LacCer displaying bilayers in 20 mM $NaNO_3$. After a 3 h incubation at room temperature, we washed each sample three times with the 20 mM $NaNO_3$ solution. The samples were then examined with an Olympus inverted fluorescence microscope, which was interfaced with a Phometrics Series 200 liquid nitrogen-cooled CCD camera. We imaged one side of each of the vesicle-coated samples, and quantified the number density of fluorescent vesicles adsorbed per unit area.

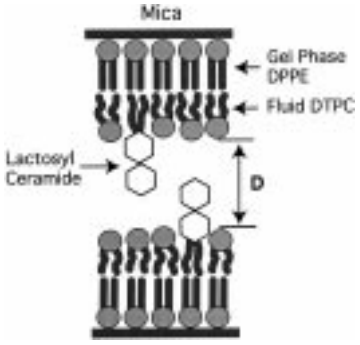

FIGURE 2: Illustration of the membrane configurations studied in this work.

RESULTS

Differential Scanning Calorimetry. Thermograms of the LacCer/DTPC dispersions were measured in water and in aqueous solutions of 20 mM sodium nitrate. In the absence of lactosyl ceramide, DTPC in water showed a single thermal event upon heating, which corresponds with the gel to liquid−crystal phase transition. The measured transition temperature of 13 °C is very close to the published value (*32*). Incorporation of 10 mol % of LacCer into DTPC decreased the melting temperature to 11 °C. This may be due to the disordering effect of the mixing process (*33*, *34*). With a mole fraction of 20% glycolipid, however, the transition temperature increased to ca. 14 °C. This is consistent with the higher melting temperature of neutral glycosphingolipids compared with zwitterionic lipids of the same hydrocarbon chain lengths (*34*, *35*). The replacement of pure water with an aqueous solution of 20 mM sodium nitrate had no effect on the melting point of the DTPC dispersion.

In any case, the changes in the DTPC melting temperature indicated that lactosyl ceramide does not phase separate when mixed with DTPC, in agreement with earlier studies (*34*). Importantly, however, all phase transition temperatures were lower than 20 °C. Thus, the monolayers of mixed lipids used in these SFA experiments were homogeneous and in the liquid−crystalline state at the experimental temperature of 25 °C.

Surface Force Measurements

Definition of Zero Interbilayer Separation. We defined the distance between the bilayer surfaces by the separation between the anhydrous headgroups of the phosphatidylcholine monolayers. Figure 2 shows the configuration of the samples used in these experiments. The steric thicknesses of the two outer lipid monolayers were determined from the difference in the distance of closest intersurface approach

following drainage of the liquid from the SFA chamber and removal of the outer lipids (*21*, *22*, *30*, *31*). The steric thickness of the hydrated lactose headgroup was then determined from the difference between the measured thickness change and the theoretical thickness of the two dehydrated DTPC layers.

We used established procedures to determine the theoretical thicknesses (*30*). For DPPE, the estimated molecular volume is 1051 Å^3. The headgroup volume is 243 Å^3, and each of the two tails in the gel phase occupies a volume of $27.4 + 26.9 \times 14 = 404$ Å^3 (*30*). This agrees closely with results obtained with the method suggested by Nagle and Wiener (*36*), which yields a molecular volume of 1071 Å^3. With the former value for the lipid volume and a mean molecular area of 43 Å^2/lipid in the deposited film, we calculated a monolayer thickness of 25 Å for DPPE in the solid phase. The DTPC monolayer was in the fluid analogous state. Thus, with a specific density of 0.76 for fluid hydrocarbon (*19*), the volume of each hydrocarbon chain is 370 Å^3. With a phosphatidylcholine headgroup volume of 324.5 Å^3, the total volume of a single DTPC phospholipid is thus 1064 Å^3. The determined mean molecular area of DTPC at a surface pressure of 35 mN/m at 25 °C is 67 Å^2. The thickness of the liquid−crystalline outer phosphocholine (PC) monolayer thus calculated is 16 Å. Contact between the outer dehydrated bilayer surfaces served as the working definition of zero separation.

The effective steric thickness of the hydrated lactosyl headgroup relative to the dehydrated PC membrane surface was determined by the interbilayer separation at the onset of the steep repulsive force, i.e., steric force, between the GSL containing lipid monolayers. The measured thickness depended on the density of sugar groups in the gap. The steric repulsion between a 10 mol % LacCer membrane and a pure DTPC layer occurred at $D < 25$ Å, and the minimum bilayer separation was 18 Å. Taking into account our measured hydration layer thickness of 6 Å on the opposed choline headgroups, the steric thickness of the hydrated disaccharide layer was thus $25 - 6 = 19$ Å. By contrast, the range of the steric force between a 20 mol % monolayer and a bare DTPC membrane increased to 31 ± 1 Å. The headgroup thickness was then $31 - 6 = 25$ Å. From molecular models, the length of the dehydrated lactosyl headgroup is 13−15 Å, depending on where the molecule resides with respect to the bilayer interface (Figure 1). These measured values suggest that the carbohydrates are fully extended from the bilayer surface in the latter case. The larger steric thickness may be due to a considerable 7−9 Å thick hydration sphere, to headgroup flexibility, or to glycolipid protrusions normal to the bilayer surface (*37*, *38*). Similarly, the minimum compressed thickness of the carbohydrate between a 10 mol % LacCer membrane and the DTPC membrane was only 12 Å $= 18 - 6$ Å, while all other measured compressed thicknesses at higher glycolipid densities were 19 Å $= 25 - 6$ Å. Thus, sparser sugar layers are thinner and slightly more compressible than denser ones.

Forces between Neutral Phosphatidylcholine Membranes. The force versus distance curve between pure DTPC monolayers is shown in Figure 3. As expected, there was no measurable force between the two DTPC monolayers at bilayer separations $D > 40$ Å. At smaller distances, the gradient of the van der Waals force exceeded the spring

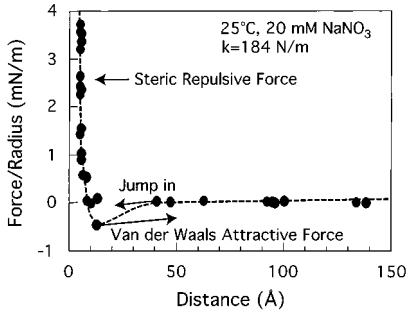

FIGURE 3: Force versus distance profiles between pure DTPC bilayers. The force profiles for the interactions between pure DTPC bilayers were measured at 25 °C in 20 mM $NaNO_3$. The jump to contact is indicated by the inward directed arrow, and the position at which the surfaces pulled apart is indicated by the outward directed arrow. The dashed line is merely to guide the eye.

Table 1. Measured Adhesion Energy and Adhesive Minimum D_0 between LacCer/DTPC Membranes in 20 mM $NaNO_3$ at 25 °C and pH 6

LacCer %	D_0 (Å)	F_j/R (mN/m)	theoretical F_j/R (mN/m)	experiment-theory
0−0	13 ± 2	−0.5 ± 0.1	−0.72	0.2
10−10	31 ± 2	−0.5 ± 0.1	−0.38	−0.1
10−20	30 ± 2	−0.7 ± 0.1	−0.51	−0.2
20−20	30 ± 3	−1.5 ± 0.2	−0.62	−0.9
30−30	31 ± 2	−3.5 ± 0.5	−0.95	−2.6
0−10	25 ± 2	−0.56 ± 0.04	−0.51	−0.05
0−20	31 ± 1	−0.5 ± 0.1	−0.70	0.2

constant, and the membranes jumped to their equilibrium separation D_0 at 13 ± 1 Å. The separation could be further decreased to the hard wall at $D = 6$ Å.

The intermembrane adhesion, determined from the pull-off force, was −0.5 ± 0.1 mN/m. The equilibrium separation at 13 ± 1 Å also corresponded to the position at which the surfaces pulled apart, or the adhesive minimum. Furthermore, there was no obvious hysteresis between the forces measured during compression versus retraction of the surfaces. This is expected, if no rearrangements of the bilayer components occur during the measurements. These data are summarized in Table 1.

From the latter minimum and the measured adhesion, we estimated the Hamaker constant between these neutral lipid bilayers from $A = (-6F\Delta D^2)/R$ (*19*, *39*). Here, R is the geometric average radius of curvature of the crossed cylinders and ΔD is the distance from the van der Waals plane of origin (*19*). Assuming that the van der Waals plane coincides with anhydrous bilayer contact, we calculated a Hamaker constant of 5×10^{-21} J. This is in good agreement with the values determined for a series of phosphatidyl cholines measured experimentally by Lis et al. (*40*).

Similarly, we determined the adhesion energy with the JKR theory for the interactions between deformable solids. According to the latter theory, the interfacial energy per area is related to the normalized adhesive force by $E = F/3\pi R$ (*19*). The determined value for pure DTPC membranes was 0.05 mJ/m^2. This value is similar to others measured between other liquid crystalline phosphocholine monolayers in aqueous solutions (*30*, *41*). Thus, the behavior of DTPC bilayers is as expected for fluid phosphatidyl choline membranes (*30*, *40*).

Measured Forces between Bare Lipid Bilayers and Membranes Displaying Lactosyl Ceramide. To investigate

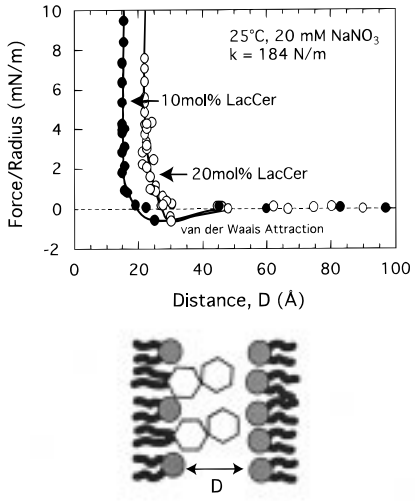

FIGURE 4: Force versus distance profiles between pure DTPC bilayers and lactosyl ceramide-containing bilayers. Forces were measured between pure phosphatidyl choline membranes and bilayers containing 10 mol % (closed circles) and 20 mol % (open circles) lactosyl ceramide. Measurements were conducted at 25 °C in 20 mM $NaNO_3$. In both cases, the membranes jumped into adhesive contact from 45 ± 5 Å. The pull-off positions are indicated by the minima in the curves. The lower panel shows the bilayer constituents and their relative configurations in these measurements.

the effect of LacCer on the interactions between bilayers, we conducted force measurements between lipid membranes containing either 10, 20, or 30 mol % LacCer. The unbuffered solutions bathing the samples were at pH 6 and 25 °C, and contained DTPC monomers and 20 mM $NaNO_3$.

We first quantified the nonspecific attraction between the glycosphingolipid-containing and lecithin membranes from the forces measured between pure DTPC and both 10 and 20 mol % LacCer bilayers. The force profile between a 10 mol % LacCer membrane and pure DTPC is shown in Figure 4 (closed circles). There was no interbilayer force until the membranes jumped into contact at $D_0 = 25$ Å from a distance of 45 ± 5 Å. At $D < 25$ Å, a soft intermembrane repulsion predominated, and the hard-wall repulsion was shifted farther from the defined anhydrous bilayer plane to 18 ± 2 Å. The latter shift was due to the steric force associated with the finite excluded volume of the protruding sugar groups and their associated waters of hydration. The steric repulsive force between these bilayers was slightly softer than that between the bare DTPC membranes.

In this case, the attractive minimum was also at 25 ± 2 Å, and the measured adhesive force was −0.56 ± 0.04 mN/m. The magnitude of the intermembrane adhesion did not decrease as might be predicted with the increased bilayer separation at pull-off. The predicted value for lipids interacting across a 25 Å aqueous gap is, for example, 0.01 mN/m, which is much smaller.

Between 20 mol % LacCer membranes and pure DTPC bilayers, the onset of the soft steric force occurred at $D <$ 31 ± 1 Å. With a spring constant of 184 N/m, the surfaces jumped into adhesive contact from 45 ± 5 Å, and the force profile exhibited a soft repulsion at 22 Å $< D <$ 30 Å. The distance of closest intermembrane approach increased slightly to 22 ± 2 Å. The ca. 8 Å range of the soft repulsion was consistent with an initially more extended headgroup configuration. Within experimental error, at −0.5 ± 0.1 mN/m, the depth of the adhesive minimum at 31 Å was similar

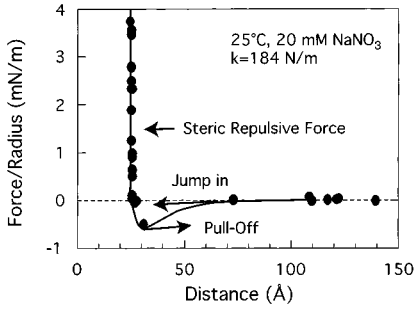

FIGURE 5: Measured forces between identical membranes containing 10 mol % lactosyl ceramide. Force measurements between 10 mol % LacCer membranes were conducted at 25 °C in 20 mM $NaNO_3$. The outward directed arrow indicates the position at which surfaces pulled apart, and the inward pointing arrow indicates the position from which the membranes jumped to adhesive contact at 31 Å. The spring constant used was 184 N/m. There was no observable difference between the forward and reverse force versus distance curves.

to that measured with the 10 mol % bilayer (Figure 4). This similarity does not preclude a small increase in the attraction, however, since the minimum was at a slightly larger bilayer separation. None of the reverse force curves exhibited hysteresis. Thus, membrane contact and separation did not induce any apparent rearrangements in the glycolipid layer. These results therefore indicate that the thickness of the carbohydrate layer depends on the glycolipid density and that the nonspecific intermembrane attraction depends only weakly on the GSL surface coverage.

The Intermembrane Attraction Increases with the Lactosyl Ceramide Surface Density. In the event of specific binding between carbohydrate headgroups, the adhesion between two membranes containing LacCer should be larger than the values reported in the previous section. We therefore measured the dependence of the interbilayer forces on the glycolipid surface density. In particular, since the nonspecific attractive interactions between GSL and lecithin membranes were relatively insensitive to the glycolipid coverage, an increase in adhesion with increasing LacCer in the opposed bilayers might provide evidence for inter-carbohydrate binding. We conducted measurements between the membranes containing the following percentages of LacCer: (A) 10 mol %−10 mol %, (B) 10 mol %−20 mol %, (C) 20 mol %−20 mol %, and (D) 30 mol %−30 mol %.

The force curve measured between identical 10 mol % LacCer membranes is shown in Figure 5. With a spring constant of 184 N/m, the bilayers jumped into contact at 31 ± 2 Å from 65 ± 5 Å. The soft repulsion at $D <$ 31 Å is as expected for the compression of the flexible GSL headgroups. The repulsive force increased steeply at $D <$ 31 ± 2 Å, and the layers could be compressed to the closest bilayer separation of 22 Å. The headgroup thickness was greater than that of individual 10 mol % LacCer bilayers, e.g., in contact with bare DTPC, but similar to the lactose on 20 mol % LacCer bilayers. Additionally, since the combined 30 Å thickness of the two contacting GSL headgroup regions was identical with that of the 20 mol % LacCer monolayer, we concluded that the opposed carbohydrate layers were interdigitated. Thus, the thickness and compressibility of the headgroup region depends on the carbohydrate concentration in the gap between the membranes. These results are summarized in Table 1.

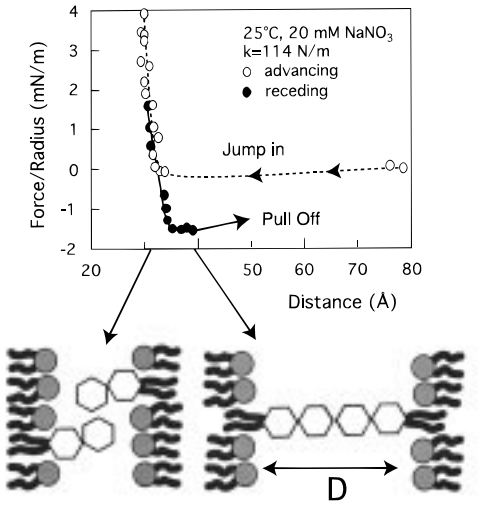

FIGURE 6: Advancing and receding force profiles measured between identical 20 mol % lactosyl ceramide bilayers. The advancing (open circles) and receding (closed circles) force profiles were measured between identical 20 mol % lactosyl ceramide membranes at 25 °C in 20 mM $NaNO_3$. Measurements were conducted with a spring constant of 114 N/m. The dashed line and inward directed arrow indicate the bilayer jump into adhesive contact at 31 ± 1 Å. The solid line shows the hysteresis in the force curve and the final pull-off position at 38 ± 2 Å. The lower panel illustrates the proposed configurations of the membrane components during these measurements.

The position of the adhesive minimum, which was measured during surface retraction, was also at 30 ± 1 Å (Table 1) and coincided with the equilibrium separation, that is, with the distance to which the surfaces jumped to contact. At −0.5 ± 0.1 mN/m, the adhesion was the same as that between the pure DTPC membrane and the 20 mol % LacCer monolayer, within experimental error. This suggested that the former attraction was due primarily to the nonspecific van der Waals force.

Increasing the GSL percentage in the bilayers to 20%, however, resulted in two notable differences in the force profiles (Figure 6) relative to those shown in Figure 5. First, the intermembrane adhesion more than doubled from −0.5 mN/m to −1.5 ± 0.3 mN/m (Table 1). Second, with a soft, more sensitive spring (k = 114 N/m), we observed a distinct hysteresis in the force curves during membrane separation. On approach, the bilayers jumped in from 75 to 31 ± 2 Å. At shorter distances, the steric repulsion predominated, and the distance of closest membrane approach was 24 ± 2 Å. In contrast, however, the final pull off did not occur at the equilibrium separation (31 Å), and the receding curve did not retrace the profile measured during approach. Rather, the bilayers detached at 38 ± 2 Å, which is 7−10 Å from the initial jump-in distance (Figure 6). By contrast, in similar measurements, i.e., k = 114 N/m, between pure DTPC and 20 mol % LacCer membranes, the forward and reverse profiles coincided (Figure 7). The latter data were devoid of any observable hysteresis.

The reverse force curves (Figure 6) indicated that the headgroups bound and that separation induced headgroup reorientations and even pulled the LacCer slightly out of the membrane before the bonds finally yielded (Figure 6, lower panel). Consistent with this, we observed that, if we halted the bilayer separation temporarily when the headgroups were apparently extended, i.e., at D > 35 Å, the membranes

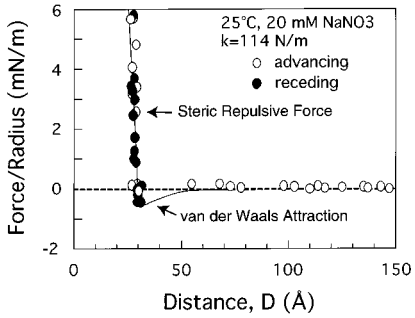

FIGURE 7: Advancing and receding force profiles between pure DTPC and a 20 mol % lactosyl ceramide membrane. The advancing (open circles) and receding (closed circles) force profiles were measured between a pure DTPC membrane and one containing 20 mol % lactosyl ceramide at 25 °C in 20 mM $NaNO_3$. Measurements were conducted with a spring constant of 114 N/m. The membranes jumped into adhesive contact at 31 ± 1 Å, and detached from the same separation.

gradually pulled back into closer contact. This occurred despite the reduced load, and indicated that the equilibrium attractive minimum was not at the final pull-off distance of 38 ± 2 Å. Because this behavior was not observed in the control measurements (Figure 7), we attribute the latter to the dynamic and, therefore, nonequilibrium, i.e., rapidly exchanging bonds between the lactose sugars.

To further investigate how the magnitude of the intermembrane adhesion scaled with the number of headgroup interactions between the bilayers, we also measured the forces between 10 and 20 mol % LacCer membranes, as well as those between identical 30 mol % LacCer bilayers. In the former case, the interbilayer carbohydrate density was intermediate between the two previous cases. Correspondingly, the measured adhesion was also intermediate between the former values at −0.7 ± 0.2 mN/m. The attractive minimum was at 31 ± 3 Å, and there was no obvious hysteresis (Table 1).

The adhesion between 30 mol % LacCer membranes was, however, much stronger at −3.5 ± 0.5 mN/m. Moreover, we readily detected hysteresis in the reverse force curves, even with a stiffer, less sensitive spring (k = 184 N/m). Consistent with this, the 30 mol % LacCer membranes also detached at 39 ± 2 Å after jumping to contact at 32 ± 1 Å. As in the measurements between 20 mol % lactosyl ceramide bilayers, the membranes tended to move back to smaller separations, if the retraction was halted before the final pull-off. This behavior is consistent with the reformation of intersurface bonds. On account of the apparent dynamic nature of the interactions, it is of interest to determine how the adhesion depends on the separation rate. We could not, however, definitively establish the time dependence of the reverse force curves. However, we attribute the greater scatter in the measured adhesion, in part, to those dynamic interactions.

Calculated van der Waals Force Between Lactosyl-Ceramide Membranes

The Net Force between Neutral Glycolipid Bilayers. To determine the molecular origins of the measured intermembrane attraction, we considered the different contributions to the forces between neutral bilayers. In the absence of attractive intercarbohydrate bonds, the net force would result

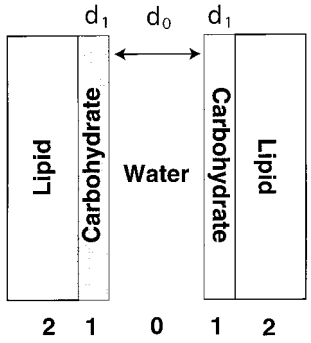

FIGURE 8: Schematic of the mixed glycosphingolipid bilayers comprising the layers shown.

from a combination of van der Waals and osmotic or steric forces. Only the van der Waals force is attractive, and the carbohydrate contribution can be obtained by subtraction of the other forces from the net measured adhesion according to

$$F_{sugar}/R = F_{exp}/R - (F_{os} + F_{vdW})/R \quad (1)$$

where F_{exp}, F_{os}, and F_{vdW} refer to the net experimentally measured, osmotic, and van der Waals forces, respectively. Because of the curved-cylinder geometry, we could not determine quantitatively the osmotic force between the membranes. Rather, we focused on calculating the attractive van der Waals contribution to eq 1.

Calculation of Hamaker Constants. We calculated the force between membranes on two opposed, crossed-cylinders of geometric average radius R. The normalized van der Waals force is $F/R = -A/6D_0^2$ where D_0 is the distance from the van der Waals plane of origin, and A is the nonretarded Hamaker constant (*19*, *30*, *39*). The Hamaker constant between two different media 1 and 2 separated by a thin film of a different material 3 (cf. Figure 8) is calculated from (*19*)

$$A_{132} = \frac{3}{4}kT\left(\frac{\epsilon_1 - \epsilon_3}{\epsilon_1 + \epsilon_3}\right)\left(\frac{\epsilon_2 - \epsilon_3}{\epsilon_2 + \epsilon_3}\right) + \frac{3h\nu_e}{8\sqrt{2}} \frac{(n_1^2 - n_3^2)(n_2^2 - n_3^2)}{(n_1^2 + n_3^2)^{0.5}(n_2^2 + n_3^2)^{0.5}\{(n_1^2 + n_3^2)^{0.5} + (n_2^2 + n_3^2)^{0.5}\}} \quad (2)$$

where ϵ_i is the static dielectric constant of each of the different layers, and n_i is the corresponding refractive index. Here, $kT = 4.114 \times 10^{-21}$ J at 25 °C, and ν_e (ca. 4×10^{15} s^{-1}) is the plasma frequency of the free electron gas (*19*). According to Figure 8, the central material could be water, but this can be altered to reflect any of the media relevant to this study. The other materials may be both lipid or lipid and carbohydrate.

With the dielectric constant of lipid $\epsilon_l = 2$ and the refractive index of lipid $n_l = 1.45$ (*37*, *41*), the calculated Hamaker constant for two lipid layers interacting across an aqueous gap is 7.3×10^{-21} J. This is close to the value of 5×10^{-21} J determined in this work. We attribute the difference between the calculated and measured values to the uncertainties both in the position of the van der Waals plane and in the refractive index of the phosphatidyl choline bilayers (*22*, *30*, *42*, *43*).

The van der Waals Force between Carbohydrate-Coated Bilayers. The presence of carbohydrate, rather than pure water, adjacent to the membrane surfaces alters the magnitude of the nonspecific van der Waals attraction between them (*26*, *44*). At 10 mol % LacCer, assuming the diameter of the hydrated sugar rings is ca. 7 Å, the carbohydrate covers 8−10% of the bilayer surface, and occupies 5 vol % or about 6 wt % of the film adjacent to the surface. The latter value was determined for an assumed 10 μm^2 region of contact between the crossed cylinders used in the force measurements (*19*). On the basis of these calculations and on electron density profiles between membranes containing 10−30 mol % GM_1 (*26*), the saccharide density is clearly nonnegligible.

In this case, the van der Waals force cannot be attributed solely to the interaction between the lipid bilayers. Rather, the net force is the summation of all contributions from the interactions between the different slabs that make up each of the interacting half-spaces (Figure 8). To calculate rigorously the force between the carbohydrate-coated membranes, we used the approach described by Israelachvili (*28*) and by Nir (*44*) for determining the van der Waals force between interacting bodies coated by multiple layers (Figure 8). In particular, the interaction force is given by

$$F = -\sum_{i=1}^{NL}\sum_{j=1}^{NR} A(i,j)H(x_{ij}) \quad (3)$$

where

$$A(i,j) = A_{ij} - A_{i-1,j} - A_{i,j-1} + A_{i-1,j-1}$$

and the A_{ij} are the Hamaker constants, which scale the interactions between species i and j across vacuum. The term $H(x)$ is a geometric parameter, which is $R/6x_{ij}^2$ for the interaction between crossed cylinders of geometric average radius R, as used in these studies. The terms x_{ij} are the distances between the different slabs. NL and NR refer to the number of layers on the left and right sides, respectively.

For the interaction between pure DTPC and LacCer-containing membranes, layer 1 on the right-hand side in Figure 8 is absent. Using accepted combining relations for the Hamaker constants (*19*, *39*, *44*) and eq 3, we obtain for the normalized force

$$\frac{F}{R} = -\frac{1}{6}\left\{\frac{A_{102}}{d_0^2} + \frac{A_{120}}{(d_0 + d_1)^2}\right\} \quad (4)$$

Here, 0, 1, and 2 refer to water, carbohydrate, and lipid, respectively. Similarly, for the symmetrical system, as illustrated in Figure 8, it can be readily shown that eq 3 for the der Waals force between two crossed-cylinders reduces to (*19*)

$$\frac{F}{R} = -\frac{1}{6}\left\{\frac{A_{101}}{d_0^2} - \frac{2A_{210}}{(d_0 + d_1)^2} + \frac{A_{212}}{(d_0 + 2d_1)^2}\right\} \quad (5)$$

In eqs 4 and 5, A_{ijk} are the Hamaker constants for materials i and k interacting across material j as calculated with eq 2.

Because the distances were small, i.e., less than 50 Å, retardation effects were not considered. For the phospholipid layers, we used a dielectric constant of 2 and a refractive index of 1.45 (*26*, *41*). The static dielectric constants of 10

Table 2. Calculated Hamaker Constants for the Interactions between the Layers Shown in Figure 8

layer parameters	212	101	210	102	120
ϵ_l (1st layer)	2	73	2	73	73
n_l (1st layer)	1.45	1.34[a]	1.45	1.34[a]	1.34[a]
		1.35[b]		1.35[b]	1.35[b]
		1.37[c]		1.37[c]	1.37[c]
ϵ_l (2nd layer)	73	80	73	80	2
n_l (2nd layer)	1.34[a]	1.33	1.34[a]	1.33	1.45
	1.35[b]		1.35[b]		
	1.37[c]		1.37[c]		
ϵ_l (3rd layer)	2	73	80	2	80
n_l (3rd layer)	1.45	1.34[a]	1.33	1.45	1.33
		1.35[b]			
		1.37[c]			
	7.06[a]	0.044[a]	−0.53[a]	0.57[a]	7.48[a]
A ($\times 10^{-21}$ J)	6.31[b]	0.15[b]	−0.86[b]	1.0[b]	7.04[b]
	5.02[c]	0.60[c]	−1.29[c]		

[a] Carbohydrate at 6 wt %. [b] Carbohydrate at 12 wt %. [c] Carbohydrate at 18 wt %.

and 20 wt % aqueous glucose and galactose solutions are 73, which is close to that of water (*45*). The refractive indices are also close to that of water at approximately 1.35 and 1.37 for 10 and 20 wt % aqueous sugar solutions, respectively (*46*). According to the calculations presented earlier in this work, the 20 wt % solution data correspond to a carbohydrate weight fraction higher than the 6−18 wt % achieved in the surface layer in these measurements. Extrapolating the refractive index data to 6, 12, and 18 wt % sugar solutions, we obtained $n = 1.34$, 1.35, and 1.37 for their respective values. The dielectric constant does not change over this concentration range.

We first determined the van der Waals force between the mixed LacCer and pure DTPC bilayers using eq 4 and coefficients determined with eq 2. With values for the 6 wt % carbohydrate film, together with those of the other materials and eq 2, the calculated values for A_{102} and A_{120} were 0.57×10^{-21} J and 7.48×10^{-21} J, respectively. The results are summarized in Table 2. The effective distances d_0 and d_1 in eq 4 were estimated on the basis of our experimental data. With 10 mol % LacCer bilayers, the jump-off distance was 25 Å from dehydrated bilayer contact. Since the cutoff distance for the van der Waals plane near the glycolipid bilayer is ca. 6 Å (*22*), $d_0 + d_1 = 25 - 6 = 19$ Å. We also assumed that d_0 corresponds to the distance between the carbohydrate layer and the dehydrated phosphocholine headgroups. Since we measured a 4−6 Å hydration layer on the DTPC membranes, we took d_0 to be 6 Å. With these distances, the Hamaker constants, and eq 4, the calculated attractive force between the pure DTPC and 10 mol % LacCer lipid films was −0.51 mN/m (Table 1). This is identical with the measured value of -0.5 ± 0.1 mN/m. Similarly, with 20 mol % LacCer, we again assumed d_0 to be 6 Å and $d_0 + d_1 = 31 - 6 = 25$ Å. Using these values, together with eq 5, and the Hamaker constants, the calculated force in this case was slightly greater at −0.70 mN/m (Table 1). This is close to the measured value of -0.5 ± 0.1 mN/m. The experimental error is ±0.1 mN/m. Furthermore, estimated errors in the calculated forces due to the uncertainties in the refractive indices are also on the order of ±0.1 mN/m. Thus, the differences between the calculated and measured values are within the limits of error.

The Hamaker constants corresponding to interactions between bilayers that both display LacCer were determined for the various terms in eq 5 relevant to the bilayer configurations investigated in this work. The Hamaker constants were determined with eq 2 and the appropriate values of the dielectric constants and refractive indices. For interactions between lecithin membranes across a 6 wt % sugar solution, $A_{212} = 7.06 \times 10^{-21}$ J. This is slightly lower than the value calculated for interactions in pure water. As shown in Table 2, decreasing the dielectric constant of the layer adjacent to the lipids, as occurs at higher saccharide densities, further decreases the magnitude of this component of the van der Waals force. The value of A_{101} was 0.04×10^{-21} J for the 6 wt % hydrated sugar slabs interacting across water. Finally, the term A_{210} for lipid and water separated by the 6 wt % carbohydrate film was -0.53×10^{-21} J. The negative sign of the latter is as expected since the refractive index and dielectric constant of the sugar layer are intermediate between that of the water and lipid (*19*, *39*). These results, as well as those values determined with the 12 and 18 wt % lactose films, are summarized in Table 2.

The effective distances d_0 and d_1 in eq 5 were estimated from both space-filling molecular models (Figure 1) and from experimental data reported previously (*21*, *22*). The origin of the van der Waals plane in water was reported previously to lie 6 Å from anhydrous bilayer contact (*22*, *30*). We therefore took $d_0 + 2d_1$, the cutoff distance for the van der Waals force between the lipids, as $31 - 6$ Å $= 25$ Å. On the basis of the model shown in Figure 1, the carbohydrate extends 11 Å beyond the van der Waals plane on each lipid layer, or $d_1 + d_0 = 14$ Å. This assigns the van der Waals plane for the carbohydrate layer to the outermost surface of lactose. The average thickness of the intervening water film d_0 was therefore 3 Å (*21*, *22*, *26*).

Using these values for the relevant distances, the data in Table 2 for 6 wt % sugar films, and eq 3, we calculated a van der Waals force between 10 mol % LacCer membranes of −0.36 mN/m (Table 1). This is essentially the same as the measured value of −0.4 mN/m. Upon increasing the glycolipid coverage, the magnitude of the terms A_{101} and A_{210} increased. The calculated attractive force between 10 and 20 mol % glycolipid membranes was −0.51 mN/m, compared with the measured value of -0.7 ± 0.1 mN/m. The calculated dispersion forces was larger between 20 mol % membranes at −0.62 mN/m, but still lower than the measured value of -1.5 ± 0.2. Finally, the measured adhesion of -3.5 ± 0.5 mN/m between 30 mol % LacCer membranes was much greater than the theoretically predicted value of −0.95 mN/m. These results are summarized in Table 1.

We then estimated the density dependence of the deviation of the measured adhesion from the theoretically predicted attractive force, neglecting any repulsive steric or osmotic contributions (Table 1). There is little difference between the calculated and measured attraction between 10 mol % LacCer bilayers. The deviation, however, increased slightly to −0.20 mN/m between 10 and 20 mol % membranes. This difference further increased to −0.9 mN/m with 20 mol % bilayers, and was even larger between 30 mol % membranes at −2.6 mN/m. The deviation from theory obviously increases with the lactose surface density. However, because osmotic and steric repulsive forces would most likely offset further density-dependent increase in adhesion at higher GSL

densities, we do not expect the adhesion to increase indefinitely with the glycolipid surface coverage.

Vesicle Adsorption Measurements

Vesicle adsorption measurements were conducted to determine whether the glycosphingolipids would alter the interactions between free bilayer membranes and supported bilayers. We also conducted control measurements of pure DTPC vesicle adsorption onto planar DTPC membranes in the absence of glycolipid. Within experimental error, there was little detectable difference observed in the number densities of adsorbed vesicles. We attribute this to the similarities in the magnitudes of the directly measured intermembrane attractive forces at the glycolipid concentrations examined. Those differences in the adhesion amount to differences in the intersurface potential between 50 and 500 nm vesicles of less than 1 kT. Thus, we did not expect to observe significant differences in the vesicle adsorption.

DISCUSSION

In these investigations, the comparison of our measurements of the adhesion between lactosyl ceramide-coated bilayers with those predicted by theory showed that the presence of the carbohydrate coat does increase the nonspecific van der Waals attraction between the membranes. This was suggested in earlier reports (*26*, *44*, *47*). Indeed, our predictions, based on Lifschitz theory, for the adhesion agreed closely with measurements between glycolipid and pure DTPC membranes, as with those between 10 mol % LacCer bilayers. However, at higher glycolipid densities, Lifschitz theory does not account for either the magnitude of or the coverage-dependent increase in the intermembrane adhesion. This latter dependence suggested that attractive interactions between the lactose headgroups, in addition to the van der Waals force, mediate the adhesion between these neutral glycosphingolipid-containing lipid membranes.

The forces measured during surface separation at high GSL densities provided direct evidence for weak binding between the carbohydrates. The bilayer separation to which the membranes first jumped into contact was 32 ± 2 Å, but the final pull-off between 20 or 30 mol % bilayers was 7−9 Å out from the initial separation. Such behavior is expected for the detachment of bound, flexible molecules (*48*, *49*). Under a tensile force, the flexible, adhering headgroups extended beyond their equilibrium configuration (Figure 6, lower panel) before they detached. In the absence of such direct adhesive contacts, there would be no driving force for headgroup extension, and pull-off would instead occur at the equilibrium separation as observed in Figures 4, 5, and 7. We further attribute the tendency of the membranes to move back to contact to an elastic-like restoring force associated with the extended glycolipids and with the dynamic reformation of intermembrane bonds. The latter dynamic interactions could pull the surfaces back into contact, as we observed, as bonds broke and reformed between the bilayers. While the differences between the "jump-in" and "pull-off" distances are not large, given the already extended configurations of the sugars, we did not expect large rearrangements. This correlation of the onset of observable hysteresis in the reverse force curves with the magnitude of the deviation between theory and the measured adhesion supports our argument that attractive interactions between carbohydrates augment the intermembrane adhesion.

The calculated magnitudes of the van der Waals forces depend on both the refractive indices and on the layer thicknesses (cf. eqs 2 and 3). We could not base our conclusions regarding the origins and magnitudes of the forces entirely on calculations, on account of the uncertainty in both the origins of the different van der Waals planes in Figure 8 and the refractive indices of the layers. Our calculations thus provide only a semiquantitative estimate of the magnitudes of the attractive van der Waals forces and therefore of the carbohydrate contribution to the adhesion.

It is, however, important to consider how different layer parameters might change the calculated van der Waals forces. For example, the use of a mass average water layer (d_0) thickness (*50*) would reduce d_1, increase d_0, and decrease the calculated force. By contrast, decreasing d_0 and increasing d_1 would increase the predicted adhesion. However, because of the physical dimensions of the lactose groups, increasing d_1 further would not be justified. The reported apparent origin of the van der Waals attraction between digalactosyl diacylglycerol (DGDG) membranes was ca. 6 Å from anhydrous bilayer contact (*22*). While we could use this value as an estimate for d_0, the latter measurement reflected primarily the largest term in eq 4 and gives no information regarding the locations of the other relevant distances. Thus, although the calculated force does depend on the estimated layer thicknesses (cf. Figure 8), the values we used were both realistic and generated larger values for the van der Waals force than other thicknesses would.

In view of the following considerations, the apparent agreement between the experimentally determined and calculated forces at the low (0−10 mol %) LacCer densities is somewhat surprising. With the sparsely grafted carbohydrate layers, the forces were measured at distances less than that between grafting sites. However, Lifschitz theory treats each of the layers as a continuum. With sparsely distributed surface groups, the discreteness of the film components cannot be neglected, and the continuum model breaks down. The force is then determined by the pairwise addition of the interactions between the lactose groups on opposed membranes (*44*, *51*). We did not use this approach due to the lack of reported excess polarizabilities for sugar molecules in water. However, Ninham and Parsegian (*51*) showed that the latter method underestimated the van der Waals force between dense hydrocarbon layers in water.

While the steric dimensions of the hydrated lactose films exceed the linear dimensions of the dehydrated sugar, our measurements agree with the measured steric thickness of the hydrated digalactosyl headgroup (*21*, *22*). On the basis of electron density profiles, membranes containing 20 mol % GM_1 in a phosphatidylcholine matrix exhibited similar carbohydrate headgroup thicknesses (*26*). This similarity is unexpected since GM_1 comprises a branched tetrasaccharide and lactose is a disaccharide. Electron density profiles of the gap between the LacCer bilayers would clearly reduce the uncertainty in our determinations of the lactose headgroup dimensions. Unfortunately, such measurements are not possible with the SFA. Additionally, it is not clear that this would enable us to better define the locations of the van der Waals planes in Figure 8.

The decrease in the headgroup thickness with decreasing GSL density is similar to the trend reported for GM_1-containing lipid mixtures (*26*). This suggests that either the headgroups tilt slightly in the absence of osmotic and steric interactions with neighboring glycolipids or that the membrane hydration increases with the surface concentration of carbohydrate (*22*). We suspect that at higher lactose densities, the increased repulsive intralayer forces caused the molecules to extend away from the surface and reduce the steric repulsion between adjacent headgroups. While such forces would reduce the intermembrane adhesion, the osmotic repulsion between the bilayers appeared to primarily reduce the compressibility of the denser carbohydrate films.

On the basis of these measurements alone, we cannot identify the chemical origins of the additional interbilayer attraction. Specific recognition between the lactose groups is unlikely. The high density of hydroxyls on the sugars, however, suggests the involvement of hydrogen bonding, which is facilitated by the close proximity of the dense lawn of lactose groups on the opposed membranes. Although the extension of the headgroups with increasing LacCer provides evidence for intermolecular repulsion, weak attractive interactions can form between close neighbors. Despite the repulsion between the opposed membranes, some bonds did nevertheless form between the carbohydrates. Thus, similar intraplanar adhesion may also occur.

Considering the extended dimensions of the lactose sugars and fluctuations normal to the bilayer surface (*38*), we expected steric overlap between the headgroups at $D < 35$ Å. That the adhesive forces apparently lock between 27 and 30 Å suggests that the LacCer headgroups may interact laterally as well as head on. The final pull-off at ca. 38 ± 2 Å further indicates that the forces between individual molecular pairs may be strong enough to tug the glycosphingolipids partially (2−3 Å) out of the bilayer. Indeed, measurements of hydrogen bond strengths between lipid-tethered nucleotides or amino acids indicated that the force to uproot the lipids is less than that needed to break hydrogen bonds (*52*, *53*). Due to the potential multivalency of the sugars, the adhesion could also involve inter- as well as intraplanar glycolipid interactions, and their collective strength could pull the glycolipids away from the opposed bilayer. That the low adhesion did not reflect significant GSL extraction (*27*), we attribute to the dynamic nature of the weak interactions. Rapidly exchanging bonds between the headgroups would rupture more frequently than the lipids uproot.

The nonlinear increase in the carbohydrate-mediated attraction with increasing lactosyl ceramide also indicates that these interactions are nonspecific and possibly cooperative. The adhesion due to stoichiometric, noncooperative binding between immobile molecules on opposed membranes would increase linearly with the bond density (*54*). Our findings further suggest that the interactions are weak and dynamic. They are insignificant at low coverage, and high carbohydrate densities are required to augment interbilayer adhesion to any appreciable extent.

The formation of attractive complexes between glycolipids on adjacent membranes or within the cell membrane has important consequences for their role in cell adhesion and in membrane organization. Such interactions could augment weak cell−cell interactions. The density-dependent forces measured in this work suggest, however, that the attraction between lactosyl headgroups is on the order of the dispersion force between pure lipid membranes. They would not be sufficiently strong to overcome entirely the electrostatic repulsion between charged membranes or to arrest cells under many conditions. Indeed, adhesion between high lactosyl ceramide expressing cells has not been observed (Hakomori, personal communication). Such attractive forces could mediate interactions between membrane components. Although the existence of such structures is controversial, glycolipid rafts might in part be stabilized by intercarbohydrate bonds (*16*). Such clusters, or rafts, have been implicated in a number of physiological functions, including protein trafficking (*16*). The physical chemical origin of the adhesion between the components is unknown, but the aggregates are robust to detergent. On account of the potential for multivalent bonding and dynamic interactions, we cannot reliably extrapolate from our force measurements to single lactose−lactose forces. These results nevertheless show that lactose headgroups can bind one another. Such interactions could play important roles in lipid organization and in GSL-mediated interactions between cell membranes.

ACKNOWLEDGMENT

We thank Prof. Brian Brandley for providing us with materials at the beginning of the project, and for helpful discussions. We also thank Prof. P. A. B. Orlean for his comments on the manuscript.

REFERENCES

1. Hakomori, S. I. (1981) *Annu. Rev. Biochem. 50*, 733−764.
2. Welply, J. K., and Jaworski, E. (1990) *Glycobiology* Wiley-Liss, New York.
3. Weis, W., and Drickamer, K. (1996) *Annu. Rev. Biochem 65*, 441−473.
4. Lowe, J. B. (1994) in *Molecular Glycobiology* (Fukuda and Hindsgaul, Eds.) pp 163−194, IRL Press, Oxford.
5. Alon, R., Hammer, D. A., and Springer, T. A. (1995) *Nature 374*, 539−542.
6. Bleil, J. D., and Wassarman, P. M. (1990) in *Glycobiology* (Welply and Jaworski, Eds.) pp 59−68, Wiley-Liss, New York.
7. Eggens, I., Fenderson, B., Toyojuni, T., Dean, B., Stroud, M., and Hakomori (1989) *J. Biol. Chem. 264*, 9476−9484.
8. Kojima, N., and Hakomori, S. I. (1991) *J. Biol. Chem. 266*, 17552−17558.
9. Hakomori, S. I. (1991) *Pure Appl. Chem. 63*, 473−482.
10. Brown, D. A., and Rose, J. K. (1992) *Cell 68*, 533−544.
11. Thompson, T. E., and Tillack, T. W. (1985) *Annu. Rev. Biophys. Chem. 14*, 361−386.
12. Krämer, E.-M., Koch, T., Niehaus, A., and Trotter, J. (1997) *J. Biol. Chem. 272*, 8937−8945.
13. Stefanova, I., Horejski, V., Ansotegui, I., Knapp, W., and Stockinger, H. (1991) *Science 254*, 1016−1020.
14. Schnitzer, J. E., McIntosh, D. P., Dvorak, A. M., Liu, J., and Oh, P. (1995) *Science 269*, 1435−1439.
15. Brown, D. A., Crise, B., and Rose, J. K. (1989) *Science 245*, 1499−1501.
16. Simons, K., and Ikonen, E. (1997) *Nature 387*, 569−572.
17. Sheets, E. D., Lee, G. M., and Jacobson, K. (1995) *Biophys. J. 68*, A306.
18. Schroeder, R., London, E., and Brown D. (1994) *Proc. Natl. Acad. Sci. 25*, 12130−12134.
19. Israelachvili, J. N. (1992) *Intermolecular and Surface Forces*, 2nd ed., Academic Press, San Diego.
20. Tamada, K., Minamikawa, H., Hato, M., and Miyano, K. (1996) *Langmuir 12*, 1666−1674.
21. Marra, J. (1985) *J. Colloid Interface Sci. 107*, 446−458.
22. Marra, J. (1986) *J. Colloid Interface Sci. 109*, 11−20.

23. Parker, J. L. (1990) *J. Colloid Interface Sci. 137*, 571−576.
24. Luckham, P., Wood, J., and Swart, R. (1993) *J. Colloid Interface Sci. 156*, 164−172.
25. Luckham, P., Wood, J., and Swart, R. (1993b) *J. Colloid Interface Sci. 156*, 173−183.
26. McIntosh, T. J., and Simon, S. A. (1994) *Biochemistry 33*, 10477−10486.
27. Leckband, D. (1995) *Nature 376*, 617−618.
28. Israelachvili, J. (1972) *Proc. R. Soc. London A 331*, 39−55.
29. Israelachvili, J. N. (1992) *Surf. Sci. Rep. 14*, 110−159.
30. Marra, J., and Israelachvili, J. (1985) *Biochemistry 24*, 4608−4618.
31. Leckband, D., Müller, W., Schmitt, F. J., and Ringsdorf, H. (1995) *Biophys. J. 69*, 1162−1169.
32. Lewis, R. N. A. H., Mak, N., and McElhaney, R. N. (1987) *Biochemistry 26*, 6118−6126.
33. Seddon, J. M., and Templer, R. H. (1993) *Philos. Trans. R. Soc. London. A 34*, 377−401.
34. Maggio, B., Ariga, T., Sturtevant, J. M., and Yu, R. K. (1985) *Biochemistry 24*, 1084−1092.
35. Maggio, B., Ariga, T., Sturtevant, J. M., and Yu, R. K. (1985b) *Biochim. Biophys. Acta 818*, 1−12.
36. Nagle, J. F., and Wiener, M. C. (1988) *Biochim. Biophys. Acta 942*, 1−10.
37. McIntosh, T. J., Magid, A. D., and Simon, S. A. (1989) *Biochemistry 28*, 7904−7912.
38. Israelachvili, J., and Wennerstrom, H. (1992) *Langmuir 6*, 873−876.
39. Hunter, R. J. (1989) *Foundations of Colloid Science*, Vol. I, Oxford Press, NY.
40. Lis, L. J., McAlister, M., Fuller, N., Rand, R. P., and Parsegian, V. A. (1982) *Biophys. J. 37*, 657−666.
41. Cherry, R. J., and Chapman, D. (1969) *J. Mol. Biol. 40*, 19−32.
42. Parsegian, V. A. (1993) *Langmuir 9*, 3625−3628.
43. Israelachvili, J. N. (1993) *Langmuir 10*, 3369−3370.
44. Nir, S. (1976) *Prog. Surf. Sci. 8*, 1−58.
45. Akhadov, Y. Y. (1980) *Dielectric Properties of Binary Solutions*, Pergamon Press, New York.
46. Lide, D. R. (1990) *Handbook of Chemistry and Physics*, 71th ed. CRC Press, Baton Rouge, LA.
47. Evans, E., and Needham, D. (1987) *J. Phys. Chem. 91*, 4219−4228.
48. Wong, J. Y., Kuhl, T., Israelachvili, J., Zalipskly, S., and Mullah, N. (1997) *Science 275*, 820−823.
49. Sheth, S., and Leckband, D. (1997) *Proc. Natl. Acad. Sci. 94*, 8399−8404.
50. LeNeveu, D. M., Rand, R. P., Parsegian, V. A., and Gingell, D. (1977) *Biophys. J. 18*, 209−230.
51. Ninham, B. W., and Parsegian, V. A. (1970) *J. Chem. Phys. 53*, 3398−3402.
52. M. Tirrell, cited with permission.
53. Pincet, F., Perez, E., Bryant, G., Lebeau, L., and Mioskowski, C. (1994) *Phys. Rev. Lett. 73*, 2780−2784.
54. Vijayendran, R., Hammer, D., and Leckband, D. *J. Chem. Phys.* (in press).

BI971010O